Global and Planetary Change 67 (2009) 78–86

Contents lists available at ScienceDirect

Global and Planetary Change

journal homepage: www.elsevier.com/locate/gloplacha

Satellite-based modeling of transpiration from the grasslands in the Southern Great Plains, USA

Joseph G. Alfieri [a], Xiangming Xiao [b], Dev Niyogi [a,c,*], Roger A. Pielke Sr. [d], Fei Chen [e], Margaret A. LeMone [e]

[a] Department of Agronomy, Crop, Soil, and Environmental Sciences, Purdue University, West Lafayette, Indiana 47907, USA
[b] Institute for the Study of Earth, Oceans, and Space, University of New Hampshire, Durham, New Hampshire 03824, USA
[c] Department of Earth and Atmospheric Sciences, Purdue University, West Lafayette, Indiana 47907, USA
[d] Colorado State University, Department of Atmospheric Science, Fort Collins, Colorado 80523, USA
[e] National Center for Atmospheric Research, Boulder, Colorado 80307, USA

ARTICLE INFO

Article history:
Accepted 8 February 2009
Available online 3 January 2009

Keywords:
Moderate Resolution Imaging Spectroradiometer (MODIS)
2002 International H2O Project
IHOP_2002
Southern Great Plains
Vegetation Transpiration Model
Vegetation Photosynthesis Model
evaporation
transpiration

ABSTRACT

Data from the 2002 International H_2O Project (IHOP_2002), which was conducted during May and June 2002 in the Southern Great Plains of the United States, was used to validate a remote sensing-based Vegetation Transpiration Model (VTM). The VTM is based on the linkage between transpiration and photosynthesis, and has been successfully tested over forest landscapes. This study is the first evaluation of the VTM model over grasslands. Since grasslands represent a significant proportion of the Earth's terrestrial surface, this research marks an important step toward applying a satellite-based transpiration model over a landscape that plays a critical role in numerous biogeochemical cycles on both regional and global scales. Comparison of the model output with observer transpiration showed the VTM tended to overestimate transpiration under sparely-vegetated conditions and overestimate transpiration when the vegetation was full. These results indicate that explicitly incorporating the effects of LAI into the VTM could improve model estimates of transpiration; they also underscore the importance of soil evaporation in grassland environments and consequently the need for a companion soil evaporation model that works with the VTM.

1. Introduction

Evapotranspiration (ET), the combined transport of moisture from the land surface to the atmosphere by soil evaporation and vegetation transpiration (TR), is a fundamental process linking numerous hydrologic, atmospheric, and ecological processes. Globally, nearly two-thirds of the precipitations that falls over land is returned to the atmosphere via ET (Baumgartner and Reichel, 1975); thus, ET is clearly an important component of the water cycle and hydrologic processes. Furthermore, as an integral component of the surface energy budget, ET is also linked to a variety of atmospheric processes (Pielke et al., 1998, 2007) ranging from the development of mesoscale circulation patterns (Hanesaik et al., 2004; Raddatz, 2007) to the evolution of the atmospheric boundary layer (LeMone et al., 2002, 2007a) and the development of convective storms (Pielke, 2001). The TR component of ET is closely connected to many ecological and biogeochemical processes ranging from nitrogen cycling (Schulze et al., 1994) to carbon uptake through photosynthesis (Farquhar and Sharkey, 1982).

Many researchers have sought to use remotely sensed data to understand and model the role of the land surface in environmental processes (e.g. Potter et al., 1993; Ruimy et al., 1994; Prince and Goward, 1995; Jiang and Islam, 2001; Norman et al., 2003; Anderson et al., 2004; Tian et al., 2004; Batra et al., 2006; Jin and Liang, 2006). This study applies a remote sensing-based photosynthesis model, the Vegetation Photosynthesis Model (VPM), and specifically the transpiration or Vegetation Transpiration Model (VTM) component of that model, over grasslands using data collected as a part of the 2002 International H_2O Project (IHOP_2002; Weckworth et al., 2004; LeMone et al., 2007b). The VTM is built on the close relationship between photosynthesis and transpiration and utilizes water use efficiency (WUE) and gross primary production (GPP) to estimate transpiration. GPP data are estimated by the VPM using satellite imagery, air temperature, and photosynthetically active radiation (PAR; Xiao et al., 2004a,b, 2005).

While the VPM and the VTM previously have been validated over forested regions (Xiao et al., 2004a,b, 2005, 2006), they have not yet been tested against observations collected over grasslands. Such a model evaluation is important because these ecosystems are a major component of terrestrial land use and land cover. Grasslands constitute approximately 52.5×10^6 km^2 or 41% of the earth's terrestrial, ice-free surface (White et al., 2000). This includes 41% of the land cover of North America (Suyker and Verma, 2001) and 22% of Europe (Soussana et al., 2007). Due to the ubiquitous nature of grasslands, they play an important role in land–atmosphere exchange

* Corresponding author. Department of Agronomy, Purdue University, 915 W. State Street, West Lafayette, Indiana 47907, USA. Tel.: +1 765 494 6574; fax: +1 765 496 2626.
E-mail address: dniyogi@purdue.edu (D. Niyogi).

0921-8181/$ – see front matter © 2008 Elsevier B.V. All rights reserved.
doi:10.1016/j.gloplacha.2008.12.003

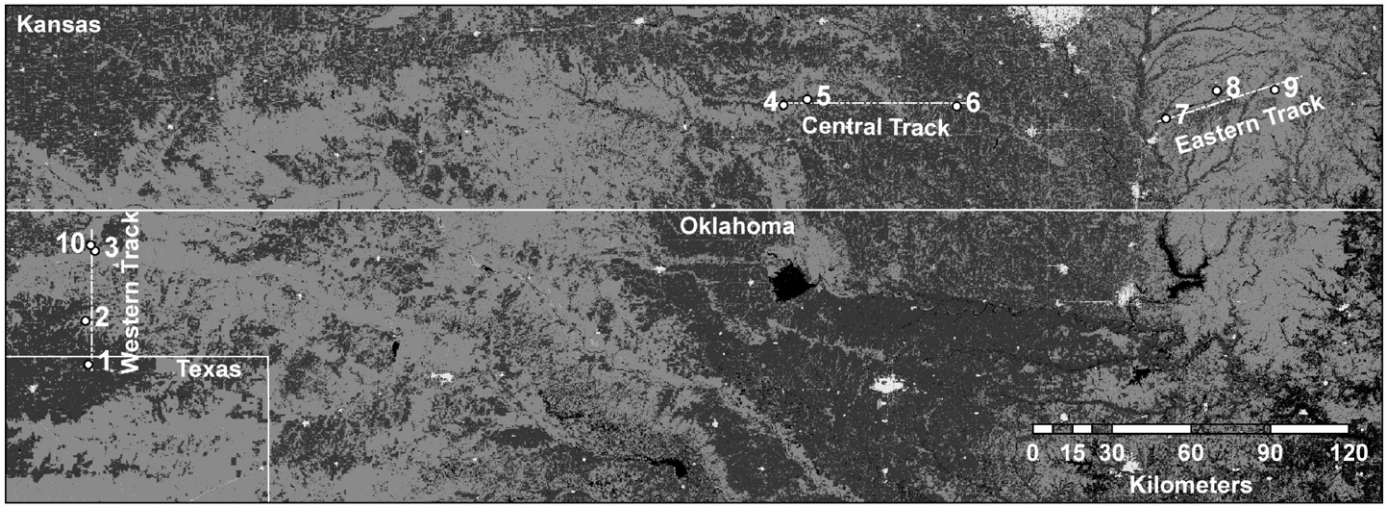

Fig. 1. The locations of the ten IHOP_2002 surface sites and their associated flight tracks are shown. The 10 surface sites can be divided into three subsets with each grouping associated with one of three flight tracks that were followed when aircraft were used to carry out atmospheric and surface observations.

processes and subsequent atmospheric phenomena (Burba and Verma, 2005).

Compared to the grasslands presented here, the forested regions used to develop the VPM and VTM models — for example, the mixed coniferous and hardwood forest at the Howland Forest Ameriflux site (Hollinger et al., 1999; Xiao et al., 2005) — have very different physical and canopy characteristics. As a result, grasslands and forested regions have very different moisture exchange characteristics; for example, grasslands tend to have a higher evaporative fraction and canopy resistance than forests (Kelliher et al., 1993). Thus, model validation is needed both to assess the skill of the VPM/VTM and to isolate those aspects of the model that would benefit from further development.

The following section briefly describes the IHOP_2002 field campaign including the surface observation sites and data collection methods. Section 3 explains the scaling scheme used to estimate transpiration from the total moisture flux observed during IHOP_2002. It also contains an overview of the VTM. Section 4 describes the results of the comparison of the modeled and observed moisture flux. Section 5 presents the conclusions drawn from the analysis.

2. Site description and data collection methods

2.1. 2002 International H_2O Project

This study used estimates of evapotranspiration derived from the observed latent heat flux measured during May and June 2002 as a part of IHOP_2002, a multi-agency field campaign conducted in the Southern Great Plains (SGP) of the United States. While a complete description of the field program is given by Weckworth et al. (2004) and LeMone et al. (2007b), a brief summary of IHOP_2002 is provided here. The research domain, which includes portions of Kansas, Oklahoma, and Texas (Fig. 1), incorporated a broad range of environmental conditions. For example, a strong west–east precipitation gradient existed across the domain. The western third of the IHOP_2002 domain experienced a protracted period of severe drought prior to and throughout the duration of the field campaign (Oklahoma Water Resource Board, 2002; LeMone et al., 2007b). The eastern third of the domain experienced a water surplus; from data available for Cowley County, Kansas, the location of the easternmost three IHOP_2002 sites, precipitation during May and June 2002 exceeded 356 mm, nearly 46% above normal (Kansas State University Weather Data Library, available at www.oznet.ksu.edu/wdl /KSPCP.htm, 2004). The research domain also represented a broad range of land cover types from bare ground and croplands (primarily winter wheat) to grasslands and sagebrush rangelands.

The field campaign included ten surface sites distributed across the IHOP_2002 domain (Fig. 1; Table 1). Each of these sites represented a combination of land use and environmental conditions that were typical of the surrounding region. As such, the sites included fallow, cropped, and grassland surfaces and dry, intermediate, and wet moisture conditions. While the analyses were conducted using all vegetated surface sites, three representative grassland sites are the focus of this paper. These three sites are Site 2, Site 4, and Site 9 (Fig. 2). Site 2 (Fig. 2a) was a sparsely-vegetated grassland site located in the panhandle of Oklahoma. A mixture of native C3 and C4 plant species that formed a mosaic of clumped vegetation and bare soil dominated Site 2. The leaf area index (LAI) — the one-sided leaf area per unit area of land surface — changed little during the field campaign; the LAI ranged from 0.15 m^2 leaf m^{-2} ground (m^2 m^{-2} hereafter) to 0.34 m^2 m^{-2} and had an average value of 0.20 m^2 m^{-2}. Similarly, this site had a greenness fraction (F_g) — the fraction of the land surface covered with green vegetation — that ranged from 0.32 at the beginning of the field campaign to a peak value of 0.44 on 16-June and 0.35 at the end of IHOP_2002. This site, which was located in the western portion of the IHOP_2002 domain, received approximately 34 mm of rain during the field campaign. Site 4 (Fig. 2b) was a grassland site located in central Kansas. The LAI and F_g at this site initially were 0.21 m^2 m^{-2} and 0.43 m^2 m^{-2}, respectively, but gradually

Table 1
The location and a summary of the environmental conditions for the 10 IHOP_2002 surface sites are shown.

Site	Location	Latitude (°N)	Longitude (°W)	Elevation (m)	Environmental Conditions
1	Booker, TX	36.4728	100.6179	872	Fallow; persistent drought
2	Elmwood, Ok	36.6221	100.6270	859	CRP grassland; persistent drought
3	Beaver, OK	36.8610	100.5945	780	Sand-sagebrush; persistent drought
4	Zenda, KS	37.3579	98.2447	509	Pasture; intermediate precipitation
5	Spivey, KS	37.3781	98.1636	506	Winter wheat; intermediate precipitation
6	Conway Springs, KS	37.3545	97.6533	417	Winter wheat; intermediate precipitation
7	New Salem, KS	37.3132	96.9387	382	Pasture; water surplus
8	Atlanta, KS	37.4070	96.7656	430	Grassland; water surplus
9	Grenola, KS	37.4103	96.5671	447	Pasture; water surplus
10	Beaver, OK	36.8701	100.6180	785	Heavily grazed pasture; persistent drought

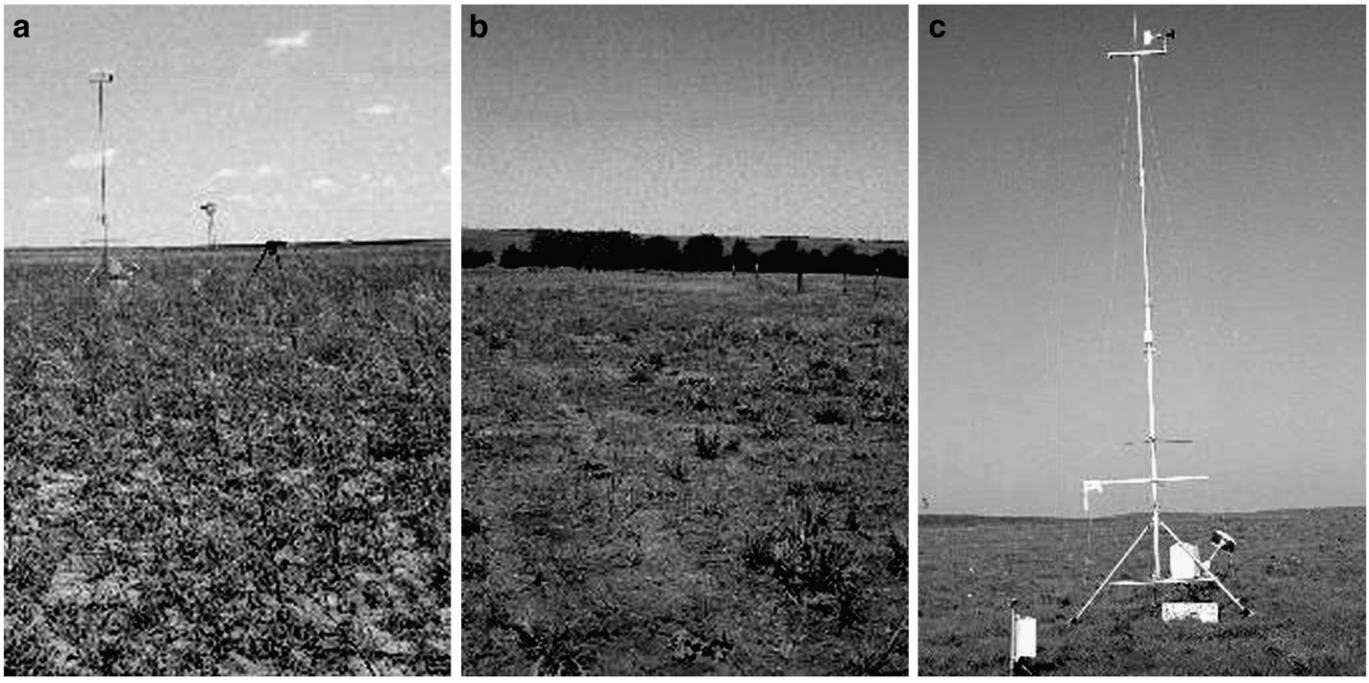

Fig. 2. Views of the three IHOP_2002 field sites that are the focus of this work presented here are shown. These sites are (a) Site 2, (b) Site 4, and (c) Site 9. Additional information and photographs of the field sites can be found at www.ral.ucar.edu/projects/land/IHOP/index.htm.

increased to plateau values 1.07 $m^2\ m^{-2}$ and 0.90 $m^2\ m^{-2}$, respectively, by mid-June. Site 4 received nearly 60 mm of rain during IHOP_2002. Site 9 (Fig. 2c) was a grassland site located within the Walnut River Watershed in southeastern Kansas. This site, which again contained a mixture of C3 and C4 species, had a LAI ranging from 0.43 $m^2\ m^{-2}$ to 2.0 $m^2\ m^{-2}$. At this site, F_g had a constant value of 1.0 during IHOP_2002. The measured rainfall at this Site 9 exceeded 117 mm for the whole of the field campaign.

2.2. Flux data collection

While a complete description of the surface data collected during IHOP_2002 may be found in LeMone et al. (2007b), a brief overview of the data used in this study is given here. The data collected included a full suite of micrometeorological, surface energy flux, and soil properties measurements (Table 2) collected on a continuous basis. The sensible (H) and latent (λE) heat fluxes were measured using the eddy covariance method. The soil moisture and temperature data were collected at a depth of 5 cm. The data were stored as 5-min block averages which were post-processed using a standard suite of corrections and aggregated to 30-min data. Also, the latent heat flux was converted to a daily total ET to facilitate comparison with the VTM output.

In order to characterize the surface conditions, periodic biophysical measurements were also made at each of the surface sites at five to ten-day intervals (Table 2). The characterization of the surface included measures of vegetation properties, such as LAI and F_g, and soil properties such as soil texture and soil moisture content (θ).

Table 2
The continuous and period observations conducted at each of the IHOP_2002 surface sites are enumerated.

Continuous	Micrometeorological measures	Air temperature; atmospheric pressure; mixing ratio; rain amount and intensity; wind speed and direction
	Radiative measures	Incident shortwave radiation; incident longwave radiation; net radiation; photosynthetic active radiation; surface temperature
	Surface energy flux	Latent heat flux; sensible heat flux; soil heat flux
	Soil properties	Soil moisture; soil temperature
Periodic	Surface characteristics	Surface soil moisture; soil type; multispectral reflectance; leaf area index; vegetation height; vegetation type

These observations include micrometeorological, radiative, surface energy flux, soil property, and surface characteristic data.

3. Evapotranspiration models

3.1. Estimation of transpiration from the IHOP_2002 data

In order to estimate the fraction of the total moisture flux measured at each of the IHOP_2002 sites that could be attributed to transpiration, the surface resistance (r_s) was first calculated using an inverted form of the Penman–Monteith (P–M) equation as follows:

$$r_s = \frac{r_a[\Delta(R_n - G) - \lambda E(\Delta - \gamma)] + \rho c_p D}{\gamma \lambda E} \quad (1)$$

where r_a is the aerodynamic resistance, Δ is the slope of the saturation vapor pressure–air temperature curve, R_n is the net radiation, G is the soil heat flux, λE is the latent heat flux, γ is the psychrometric constant, ρ is the air density, c_p is the specific heat, and D is the vapor pressure deficit. The canopy resistance (r_c) was then derived from r_s by scaling r_s as a function LAI following the method developed by Hatfield and Allen (1996). Using this method r_c is estimated as follows:

$$r_c = \frac{0.3\mathrm{LAI} + 1.2}{\mathrm{LAI}} r_s \quad (2)$$

Finally, the component of λE associated with transpiration was calculated by inserting this estimate of r_c back into the P–M equation.

$$\lambda E_{TR} = \frac{(R_n - G) + \frac{\rho c_p D}{r_a}}{\Delta + \gamma\left(\frac{r_c}{r_a} - 1\right)} \quad (3)$$

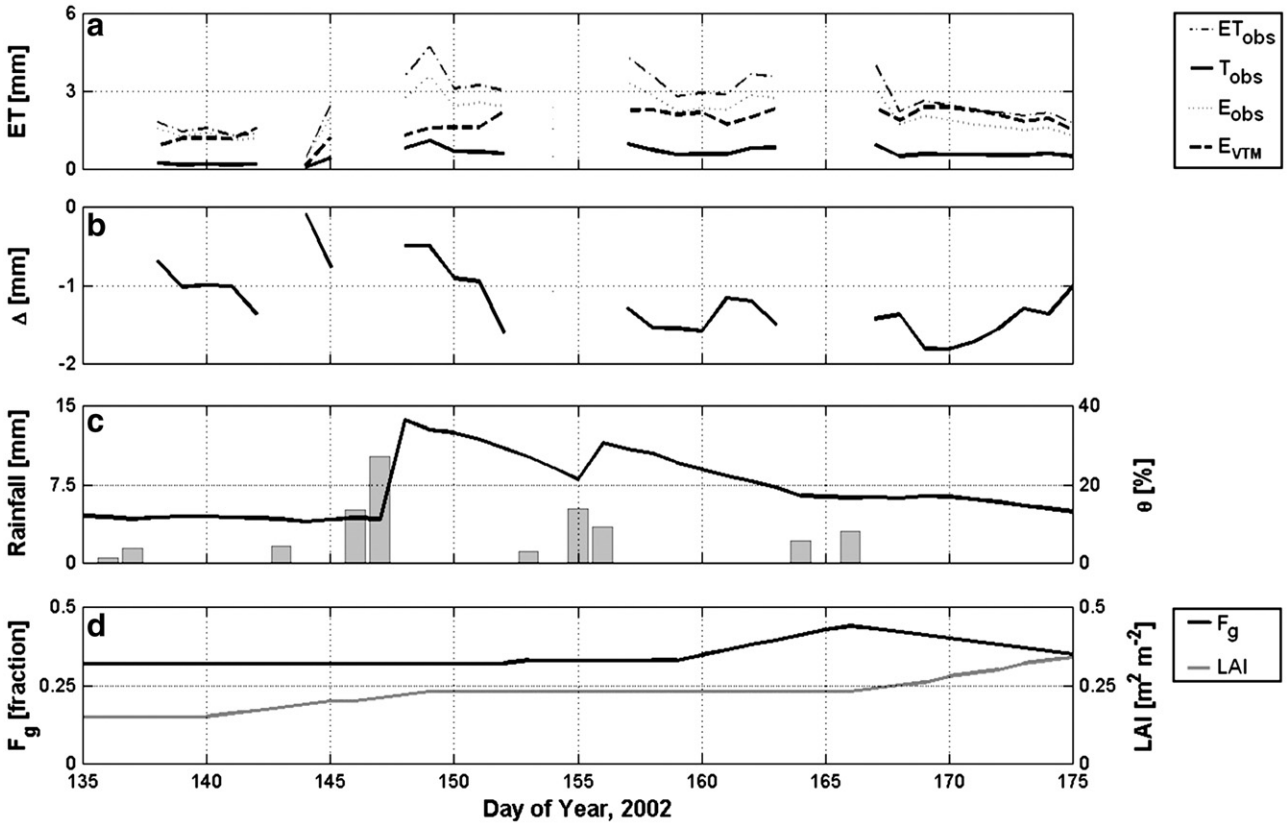

Fig. 3. The observed and modeled moisture flux (a), difference between the observed and modeled transpiration (b), rainfall amount and soil moisture content (c), and greenness fraction and leaf area index (d) are shown for Site 2.

Since this technique cannot account for the evaporation of water intercepted by the canopy or ponded at the surface, only days without rainfall were considered for further analysis.

3.2. The VTM model

The VTM combines WUE and GPP to estimate TR. In brief, TR is estimated by scaling GPP by δ_g as follows:

$$\mathrm{TR} = \delta_g \times \mathrm{GPP} \tag{4}$$

where δ_g is WUE (μmol H_2O/μmol CO_2). At leaf level, $\delta_g = 500$ (μmol H_2O/μmol CO_2) for C3 plants and $\delta_g = 250$ (μmol H_2O/μmol CO_2) for C4 plants (Taiz and Zeiger, 2002).

GPP is estimated from the Vegetation Photosynthesis Model (VPM) as

$$\mathrm{GPP} = \varepsilon_g \times \mathrm{FPAR}_{\mathrm{chl}} \times \mathrm{PAR} \tag{5}$$

where ε_g is the light use efficiency (μmol CO_2/μmol PAR), $\mathrm{FPAR}_{\mathrm{chl}}$ is the fraction of PAR absorbed by leaf chlorophyll, and PAR is the photosynthetically active radiation. The detailed description of the VPM model is given in other papers (Xiao et al., 2004a,b, 2005, 2006); a brief review is presented here.

The VPM model uses two vegetation indices: the enhanced vegetation index (EVI; Huete et al., 1997) and the land surface water index (LSWI; Xiao et al., 2004a). EVI is defined as

$$\mathrm{EVI} = 2.5 \times \left[\frac{\rho_{\mathrm{nir}} - \rho_{\mathrm{red}}}{\rho_{\mathrm{nir}} + (6\rho_{\mathrm{red}} - 7.5\rho_{\mathrm{blue}}) + 1}\right] \tag{6}$$

where ρ_{nir} is the near infrared reflectance, ρ_{red} is the red reflectance, and ρ_{blue} is the blue reflectance at the surface. LSWI is defined as

$$\mathrm{LSWI} = \frac{\rho_{\mathrm{nir}} - \rho_{\mathrm{swir}}}{\rho_{\mathrm{nir}} + \rho_{\mathrm{swir}}} \tag{7}$$

where ρ_{swir} is the shortwave infrared reflectance. EVI is used as a proxy for $\mathrm{FPAR}_{\mathrm{chl}}$ and LSWI is used to calculate the light use efficiency (ε_g).

The light use efficiency is defined as

$$\varepsilon_g = \varepsilon_0 \times T_{\mathrm{scalar}} \times W_{\mathrm{scalar}} \times P_{\mathrm{scalar}} \tag{8}$$

where ε_0 is the maximum light use efficiency, and T_{scalar}, W_{scalar}, and P_{scalar} are down-regulation scaling factors for the effects of temperature, water, and leaf phenology on light use efficiency.

Each of the scaling factors can be determined utilizing either surface observational data or remotely-sensed data. The scaling factor for temperature effects, which was developed for the Terrestrial Ecosystem Model (Raich et al., 1991), is calculated as

$$T_{\mathrm{scalar}} = \frac{(T - T_{min})(T - T_{max})}{[(T - T_{min})(T - T_{max})] - \left(T - T_{\mathrm{opi}}\right)^2} \tag{9}$$

where T is the air temperature, and T_{min}, T_{max}, and T_{opt} are the minimum, maximum, and optimum temperatures for photosynthetic activity, respectively. The scaling factor for water is derived from the LSWI as:

$$W_{\mathrm{scalar}} = \frac{1 + \mathrm{LSWI}}{1 + \mathrm{LSWI}_{max}} \tag{10}$$

where $LSWI_{max}$ is the maximum LSWI value within the plant growing season. Finally, the scaling factor for leaf phenology is:

$$P_{scalar} = \frac{1 + LSWI}{2} \quad (11)$$

prior to full expansion of the leaf and

$$P_{scalar} = 1 \quad (12)$$

after full expansion of the leaf. For the purposes of this study, which uses data collected during the summer months, P_{scalar} is held constant as 1.

4. Results

4.1. IHOP_2002 Site 2

Over the rain-free days during the whole of the IHOP_2002 field campaign, the total observed ET and TR were 80.6 mm and 17.2 mm, respectively. The sum of the modeled TR from the VTM for the same period, which was more than three times the TR derived from the observations, was 54.5 mm. On a daily basis, the difference between the observed and modeled TR (Δ) was approximately 1.25 mm, however, the magnitude of this difference varied over time (Fig. 3). By plotting Δ as a function of θ (Fig. 4), it can be seen that the data is well correlated ($r = 0.82$). While θ is not considered directly by the VTM, θ may impact the VTM through its influence on the LSWI. The shortwave infrared reflectance used to calculate LSWI is sensitive to both the moisture content of the vegetation and the soil (Xiao et al., 2002). Given the sparse vegetation cover at Site 2, the signal from the bare surface most likely corrupts the shortwave infrared reflectance measurement, thus the estimate of LSWI. Since LSWI is used in the calculation of both W_{scalar} and P_{scalar}, any error in determining LSWI would propagate through to the modeled TR.

4.2. IHOP_2002 Site 4

The observed and modeled TR for Site 4 were 34.3 mm and 25.1 mm, respectively. Although the 9.1 mm difference between these values is substantially lower than the 37.3 mm difference between the modeled and observed TR at Site 2, the VTM still fails to capture the observed TR (Fig. 5). While the difference in TR values can again be linked to θ, LAI is also influential at this site. For values of LAI less than 0.5, the VTM tends to overestimate TR, on average by 1.2 mm d^{-1}. Furthermore, under these more sparsely-vegetated conditions, a similar, albeit less well-defined, relationship exists between Δ and θ (Fig. 6). When LAI exceeded 0.9, the VTM underestimated TR by an average of 2.1 mm d^{-1}. The magnitude of the underestimate is proportional to θ.

4.3. IHOP_2002 Site 9

At Site 9, the total TR derived from the observational data was 85 mm or 87% of the total ET (99 mm) measured at the site. In contrast, the VTM, which calculated a total TR of only 24 mm, underestimated TR by as much as 4.3 mm d^{-1}. As was the case at Site 4, the error in VTM can be linked to θ and LAI at Site 9 (Fig. 7). When LAI was low, i.e. less than 0.5 m^2 m^{-2}, Δ is weakly correlated with θ (Fig. 8); however, the range in θ was too small to demonstrate a clear pattern such as was found at the other IHOP_2002 sites. At the higher values of LAI, which ranged from 0.67 m^2 m^{-2} to 2.0 m^2 m^{-2}, Δ was poorly correlated with θ. However, the range in θ was again limited to near-saturation conditions (Fig. 8). As can be seen in Fig. 9, the difference is strongly correlated to LAI ($r = 0.92$). This result points out

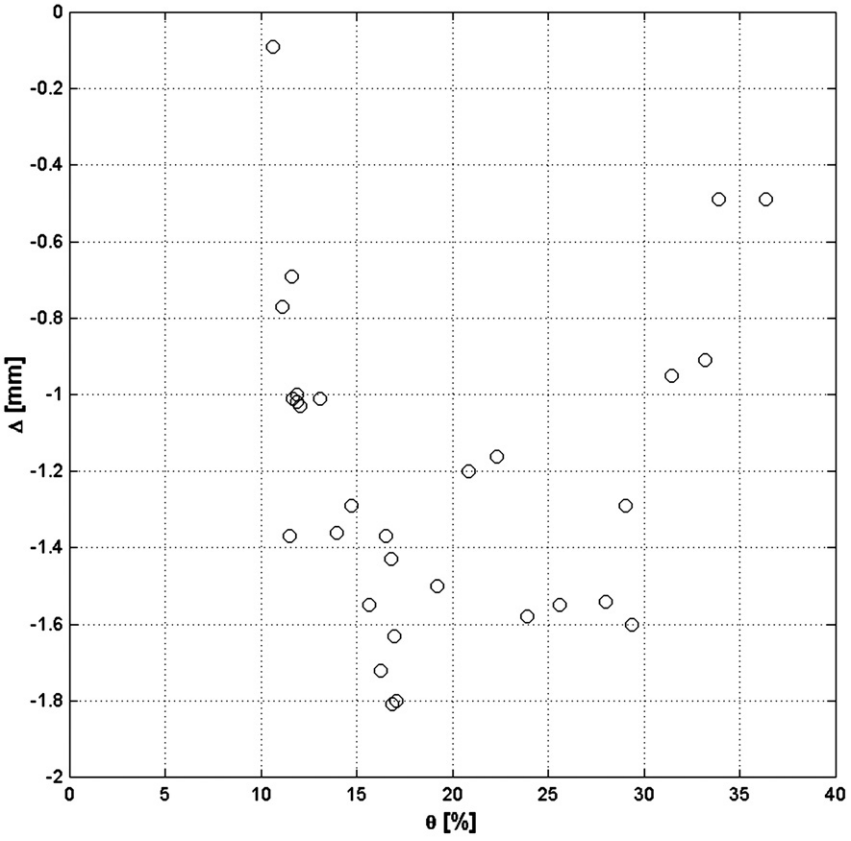

Fig. 4. The relationship between the difference in modeled and observed transpiration and soil moisture content is shown for Site 2.

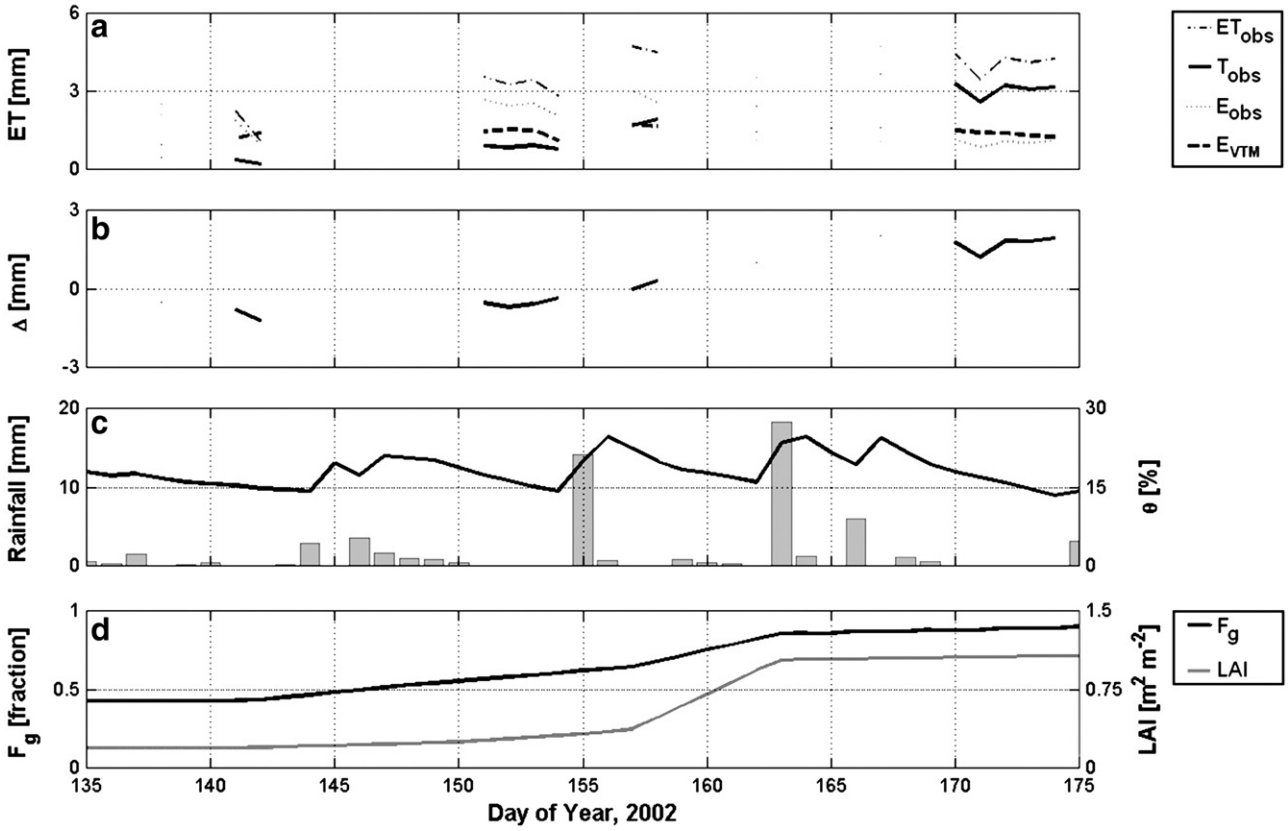

Fig. 5. The observed and modeled moisture flux (a), difference between the observed and modeled transpiration (b), rainfall amount and soil moisture content (c), and greenness fraction and leaf area index (d) are shown for Site 4.

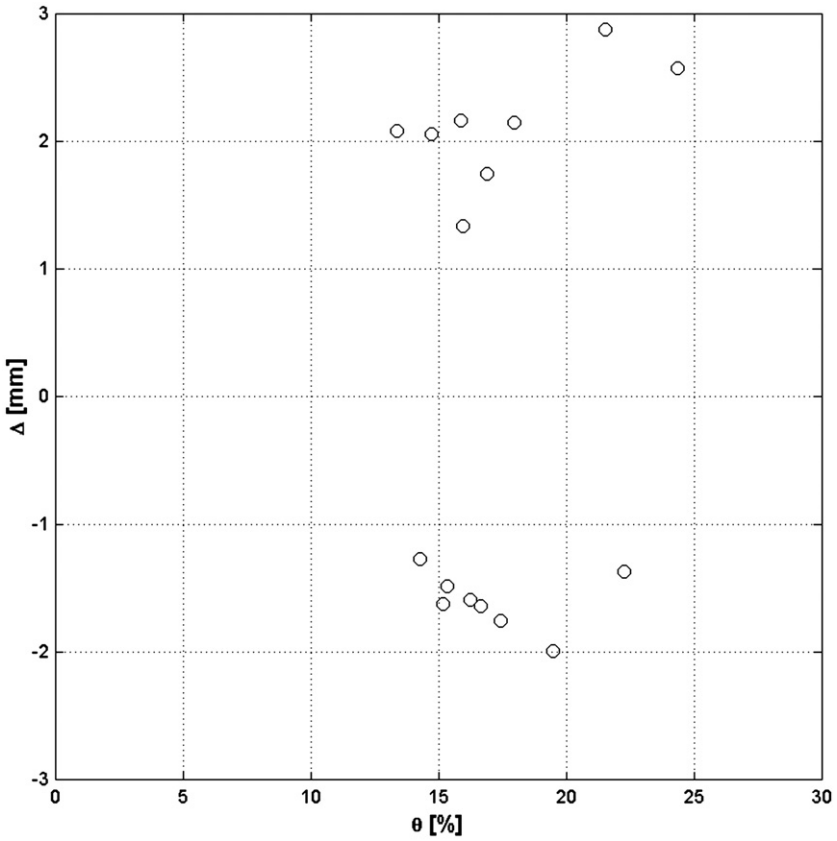

Fig. 6. The relationship between the difference in modeled and observed transpiration and soil moisture content is shown for Site 4.

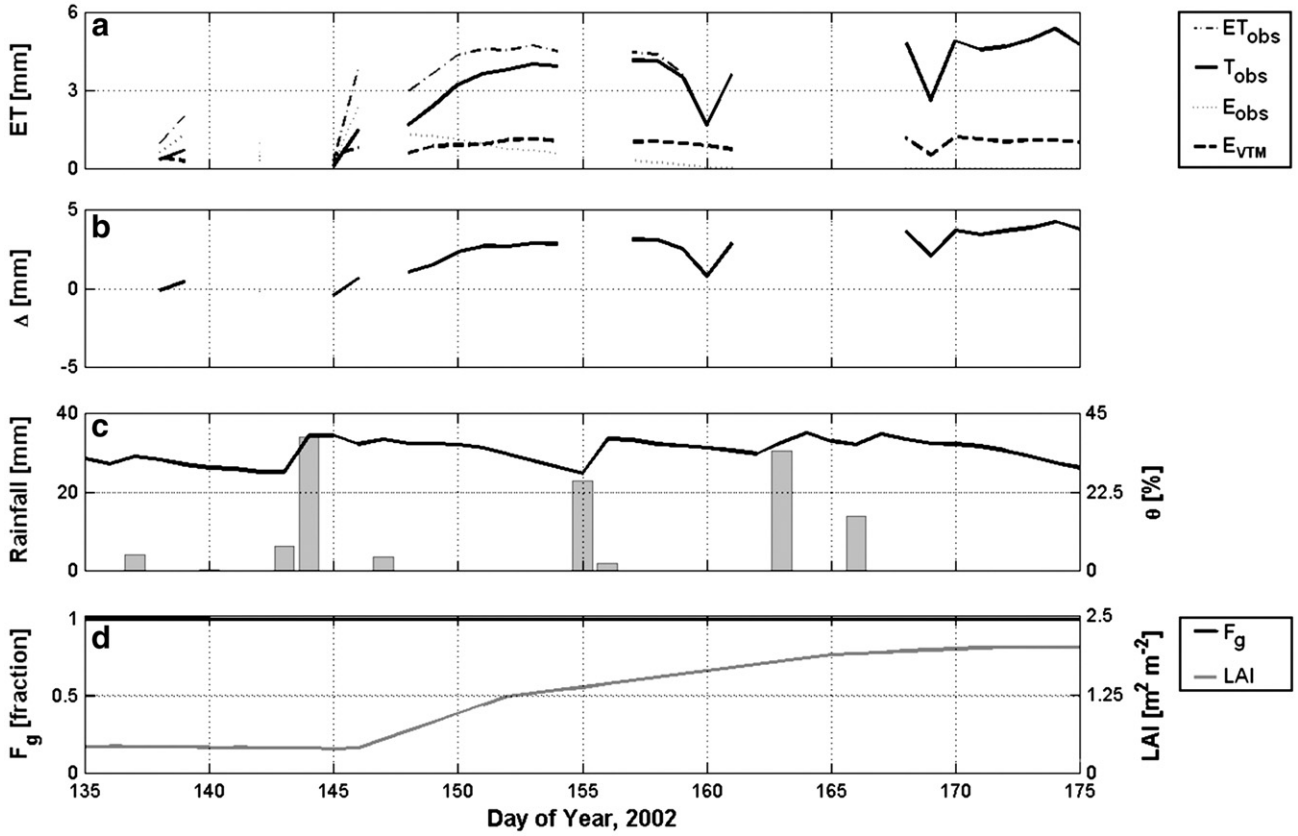

Fig. 7. The observed and modeled moisture flux (a), difference between the observed and modeled transpiration (b), rainfall amount and soil moisture content (c), and greenness fraction and leaf area index (d) are shown for Site 9.

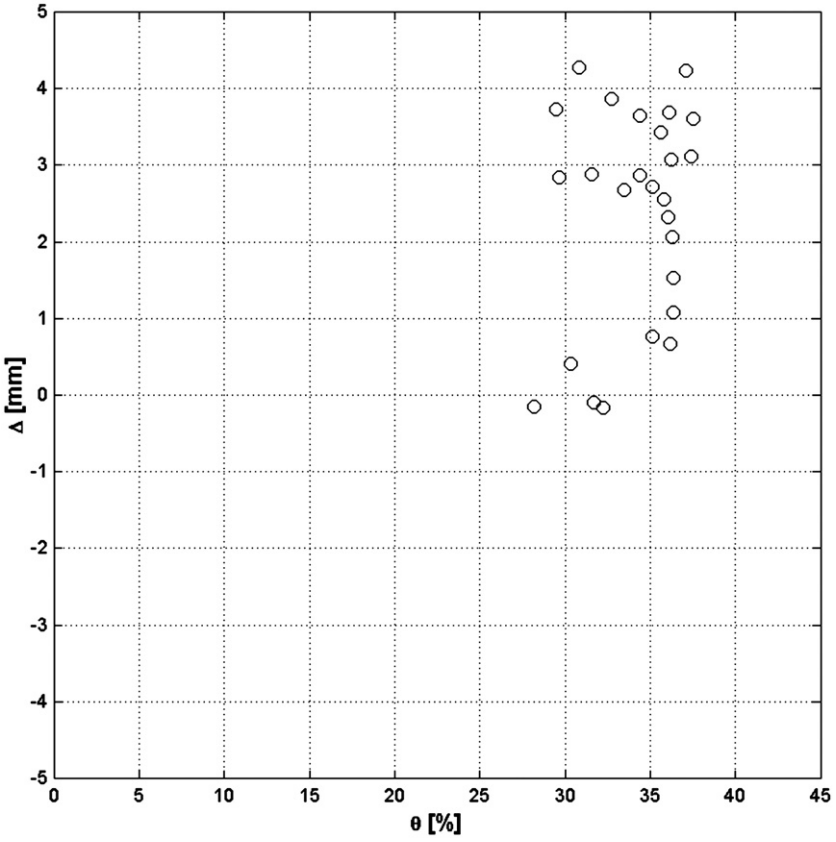

Fig. 8. The relationship between the difference in modeled and observed transpiration and soil moisture content is shown for Site 9.

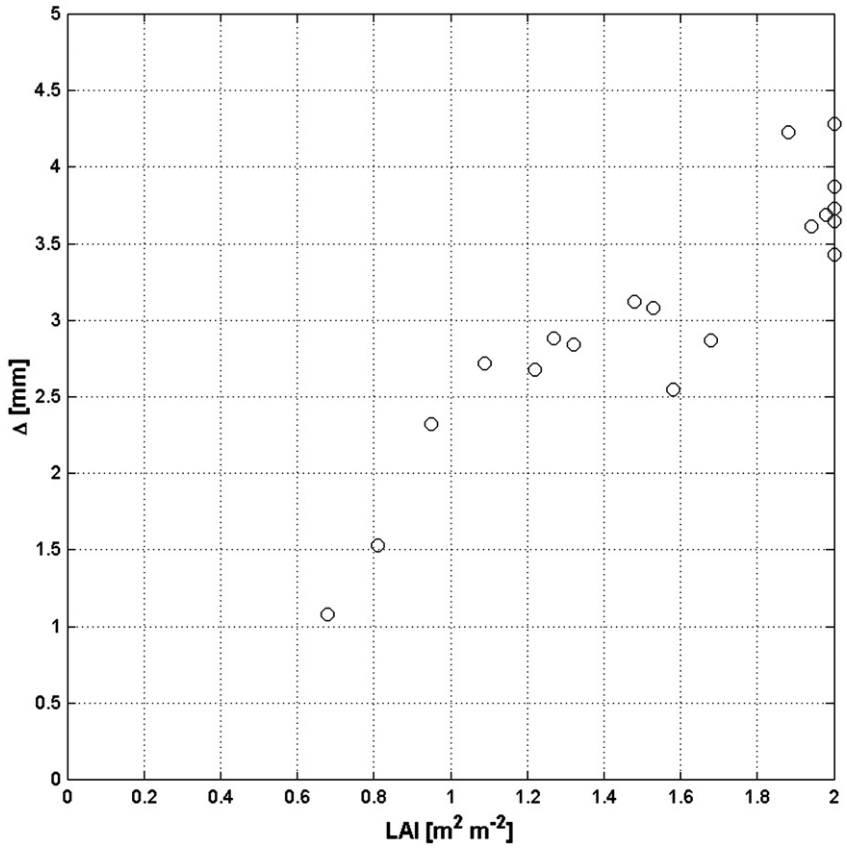

Fig. 9. The relationship between the difference in modeled and observed transpiration and leaf area index is shown for Site 9.

both the importance of LAI in characterizing TR in grasslands and a second potential shortcoming of using the VTM over grasslands: the model does not explicitly consider the effects of LAI.

5. Conclusions

The results of this study suggest the MODIS-based VTM model reproduce the observed TR from grasslands poorly. The model tends to overestimate TR under sparsely vegetated conditions and underestimate TR at high values of LAI. When the vegetation is sparse, i.e. there is a low LAI, the characteristics of the exposed soil — for example, moisture content — could influence LSWI. An inaccurate estimate of LSWI would propagate into the estimate of TR by the VTM. When the vegetation is full, the underestimate is directly related to LAI. In both cases, the explicit consideration of LAI in the model could improve the VTM's ability to model TR over grasslands.

An additional limitation of the model that could impact its ability to estimate TR over grasslands is the assumption of a constant WUE. While this assumption may be reasonable at the leaf level, it could be problematic at ecosystem scales and could contribute to the overestimate of moisture exchange by the VTM. As such, the discrepancy between the observed and modeled moisture flux indicates the need for further development of the VTM. Specifically, an improved representation of the diurnal and inter-seasonal variability in WUE could enhance the model's ability to reproduce the TR observed over grasslands.

A third limitation of the VTM is that it uses a relatively simplistic expression (Eq. (4)) to estimate TR. As a result, it does not explicitly consider the environmental factors (e.g. incident solar radiation, air temperature, humidity, plant phenology, etc.) that can have a substantial influence on TR (Alves and Pereiera, 2000; Alfieri et al., 2007a). For example, Alfieri et al. (2007b) showed for the grasslands in the IHOP_2002 domain TR is closely linked to changing species distribution and plant phenology. As a result, the VTM is not able to reproduce the short-term variability in TR that is linked to changing environmental conditions. This could impact both the daily estimates of TR by the VTM and longer term water budgets derived from model data.

The results of this study also underscore the importance of soil evaporation in grassland environments. Particularly at the sparsely vegetated sites, soil evaporations accounted for as much as 80% of ET. Thus, in order to fully capture moisture exchange in grasslands with a remote sensing model, a soil evaporation model is needed that can be used in conjunction with the VTM.

Acknowledgments

The authors would like to thank M. O'Connell for her assistance during the course of this research. The authors would like to acknowledge Dr. S. Nelson and NSF (ATM 0233780; ATM 0236885; ATM 0296159), Dr. J Entin and NASA-THP (NNG04GI84G), and Drs. J. Entin and G. Gutman and NASA-IDS (NNG04GL61G), USDA NRICGP (Water Resources, through Tufts University, S. Islam) and NASA Land Use Land Cover Change Program for support of this research.

References

Alfieri, J.G., Blanken, P.D., Yates, D.N., Steffen, K., 2007a. Variability in the environmental factors driving evapotranspiration from a grazed rangeland during severe drought conditions. Journal of Hydrometeorology 8, 207–220.

Alfieri, J.G., Niyogi, D., Blanken, P.D., Chen, F., LeMone, M.A., Ek, M., Mitchell, K., Kumar, A. 2007b. Estimation of minimum canopy resistance for croplands and grasslands. Journal of Applied Meteorology and Climatology, in review.

Alves, I., Pereiera, L.S., 2000. Modeling surface resistance from climatic variables? Agricultural Water Management 42, 371–385.

Anderson, M.C., Norman, J.M., Mecikalski, J.R., Torn, R.D., Kustas, W.P., Basara, J.B., 2004. A multiscale remote sensing model for disaggregating regional fluxes to micrometeorological scales. Journal of Hydrometeorology 5, 343–363.

Batra, N., Islam, S., Venturini, V., Bisht, G., Jiang, L., 2006. Estimation and comparison of evapotranspiration from MODIS and AVHRR sensors for clear sky days over the Southern Great Plains. Remote Sensing of Environment 103, 1–15.

Baumgartner, A., Reichel, E., 1975. The World Water Balance. Elsevier. 179 pp.

Burba, G.G., Verma, S.B., 2005. Seasonal and interannual variability in evapotranspiration of native tallgrass prairie and cultivated wheat ecosystems. Agricultural and Forest Meteorology 135, 190–201.

Farquhar, G.D., Sharkey, T.D., 1982. Stomatal conductance and photosynthesis. Annual Reviews of Plant Physiology 33, 317–345.

Hanesaik, J.M., Raddatz, R.L., Lobban, S., 2004. Local initiation of deep convection on the Canadian prairie provinces. Boundary-Layer Meteorology 110, 455–470.

Hatfield, J.L., Allen, R.G., 1996. Evapotranspiration estimates under deficient water supplies. Journal of Irrigation and Drainage Engineering 122, 301–308.

Hollinger, D.Y., Goltz, S.M., Davidson, E.A., Lee, J.T., Tu, K., Valentine, H.T., 1999. Seasonal patterns and environmental control of carbon dioxide and water vapour exchange in an ecotonal boreal forest. Global Change Biology 5, 891–902.

Huete, A.R., Liu, H.Q., Batchily, K., van Leeuwen, W., 1997. A comparison of vegetation indices global set of TM images for EOS MODIS. Remote Sensing of Environment 59, 440–451.

Jiang, L., Islam, S., 2001. Estimation of surface evaporation map over Southern Great Plains using remote sensing data. Water Resources Research 37, 329–340.

Jin, M.L., Liang, S., 2006. An improved land surface emissivity parameter for land surface models using global remote sensing observations. Journal of Climate 19, 2867–2881.

Kelliher, F.M., Leuning, R., Schulze, E.D., 1993. Evaporation and canopy characteristics of coniferous forests and grasslands. Oecologia 95, 153–163.

LeMone, M.A., Grossman, R.L., McMillen, R.T., Liou, K.-N., Ou, S.C., McKeen, S., Angevine, W., Ikeda, K., Chen, F., 2002. CASES-97: late-morning warming and moistening of the convective boundary layer over the Walnut River Watershed. Boundary-Layer Meteorology 104, 1–52.

LeMone, M.A., Chen, F., Alfieri, J.G., Tewari, M., Geerts, B., Miao, Q., Grossman, R.L., Coulter, R.L., 2007a. Influence of land cover, soil moisture, and terrain on the horizontal distribution of sensible and latent heat fluxes and boundary layer structure in southeast Kansas during IHOP_2002 and CASES-97. Journal of Hydrometeorology 8, 68–87.

LeMone, M.A., Chen, F., Alfieri, J.A., Cuenca, R., Niyogi, D., Kang, S., Davis, K., Blanken, P.D., 2007b. Surface, soil, and vegetation network during the international H_2O project 2002 field campaign. Bulletin of the American Meteorological Society 88, 65–81.

Norman, J.M., Anderson, M.C., Kustas, W.P., French, A.N., Mecikalski, J., Torn, R., Diak, G.R., Schmugge, T.J., 2003. Remote sensing of surface energy fluxes at 10(1)-m pixel resolutions. Water Resources Research 38. doi:10.1029/2002WR001775.

Oklahoma Water Resource Board, 2002. July 3 Oklahoma Water Resources Bulletin and Summary of Current Conditions. Oklahoma Water Resource Board. [Available from Oklahoma Water Resources Board, 3800 N. Classen Blvd., Oklahoma City, OK 73118.].

Pielke, R.A., 2001. Influence of the spatial distribution of vegetation and soils on the prediction of cumulus convective rainfall. Reviews of Geophysics 39, 151–177.

Pielke, R.A., Avissar, R., Raupach, M., Dolman, A.J., Zeng, X.B., Denning, A.S., 1998. Interactions between the atmosphere and terrestrial ecosystems: influence on water and climate. Global Change Biology 4, 461–475.

Pielke, R.A. Sr., Adegoke, J., Beltran-Przekurat, A., Hiemstra, C.A., Lin, J., Nair, U.S., Niyogi, D., Nobis, T.E., 2007. An overview of regional land use and land cover impacts on rainfall. Tellus B 59, 587–601.

Potter, C.S., Randerson, J.T., Field, C.B., Matson, P.A., Vitousek, P.M., Mooney, H.A., Klooster, S., 1993. Terrestrial ecosystem production: a process model based on global satellite and surface data. Global Biogeochemical Cycles 7, 811–841.

Prince, S.D., Goward, S.N., 1995. Global primary production: a remote sensing approach. Journal of Biogeography 22, 815–825.

Raddatz, R.L., 2007. Evidence for the influence of agriculture on weather and climate through the transformation and management of vegetation: illustrated by examples from the Canadian Prairies. Agricultural and Forest Meteorology 142, 186–202.

Raich, J.W., Rastetter, E.B., Melillo, J.M., Kicklighter, D.W., Steudler, P.A., Peterson, B.J., 1991. Potential net primary productivity in South-America-application of a global-model. Ecological Applications 1, 399–429.

Ruimy, A., Saugier, B., Dedieu, G., 1994. Methodology for the estimation of terrestrial net primary production from remotely sensed data. Journal of Geophysical Research 99, 5263–5283.

Schulze, E.D., Kelliher, F.M., Körner, C., Lloyd, J., Leuning, R., 1994. Relationships among maximum stomatal conductance, ecosystem conductance, carbon assimilation rate, and plant nitrogen nutrition: a global ecology scaling exercise. Annual Review of Ecology and Systematics 25, 629–660.

Soussana, J.F., et al., 2007. Full accounting of the greenhouse gas (CO_2, N_2O, CH_4) budget of nine European grassland sites. Agricultural Ecosystems and Environment 121, 121–134.

Suyker, A.E., Verma, S.B., 2001. Year-round observations of the net ecosystem exchange of carbon dioxide for a native tallgrass prairie. Global Change Biology 7, 279–289.

Tian, Y., Dickinson, R.E., Zhou, L., Shaikh, M., 2004. Impact of a new land boundary conditions for Moderate Resolution Imaging Spectroradiometer (MODIS) data on the climatology of land surface variables. Journal of Geophysical Research 109. doi:10.1029/2004JD005443.

Taiz, L., Zeiger, E., 2002. Plant Physiology, 3rd Edition. Sinauer Associates. 690 pp.

White, R., Murray, S., Rohweder, M., 2000. Pilot Analysis of Global Ecosystems: Grassland Ecosystems. World Resources Institute, Washington D.C.

Weckworth, T.M., Parsons, D.B., Koch, S.E., Moore, J.A., LeMone, M.A., Demoz, B., Flamant, C., Geerts, B., Wang, J., Feltz, W.F., 2004. An overview of the International H_2O Project (IHOP 2002) and some preliminary highlights. Bulletin of the American Meteorological Society 85, 253–277.

Xiao, X., Boles, S., Liu, J.Y., Zhuang, D.F., Liu, M.L., 2002. Characterization of forest types in Northeastern China, using multitemporal SPOT-4 VEGETATION sensor data. Remote Sensing of Environment 82, 335–348.

Xiao, X., Hollinger, D., Aber, J.D., Goltz, M., Davidson, E.A., Zhang, Q.Y., 2004a. Satellite-based modeling of gross primary production in an evergreen needleleaf forest. Remote Sensing of Environment 89, 519–534.

Xiao, X., Zhang, Q., Braswell, B., Urbanski, S., Boles, S., Wofsy, S.C., Moore, B.I., Ojima, D., 2004b. Modeling gross primary production of a deciduous broadleaf forest using satellite images and climate data. Remote Sensing of Environment 91, 256–270.

Xiao, X., Zhang, Q., Hollinger, D., Aber, J., Moore, B., 2005. Modeling gross primary production of an evergreen needleleaf forest using MODIS and climate data. Ecological Applications 15, 954–969.

Xiao, X., Hagen, S., Zhang, Q., Keller, M., Moore, B., 2006. Detecting leaf phenology of seasonally moist tropical forests in South America with multi-temporal MODIS images. Remote Sensing of Environment 103, 465–473.